

Methods cooperation for multiresolution motion estimation

Rémy Leconge

Olivier Laligant

Frédéric Truchetet, MEMBER SPIE

Alain Diou

Université de Bourgogne

Le2i

France

E-mail: r.leconge@iutlecreusot.u-bourgogne.fr

Abstract. For a medical application, we are interested in an estimation of optical flow on a patient's face, particularly around the eyes. Among the methods of optical flow estimation, gradient estimation and block matching are the main methods. However, the gradient-based approach can only be applied for small displacements (one or two pixels). Generally, the process of block matching leads to good results only if the searching strategy is judiciously selected. Our approach is based on a Markov random field model, combined with an algorithm of block matching in a multiresolution scheme. The multiresolution approach allows detection of a large range of speeds. The large displacements are detected on coarse scales and small displacements are detected successively on finer scales in a coarse to fine strategy. The Markov random fields allow the initialization and control of motion estimation across all scales. The tracking of motion is achieved by a block matching algorithm. This method gives the optical flow, whatever the amplitude of motion is, if pertaining to the range defined by the multiresolution approach. The results clearly show the complement of Markov random field estimation and block matching across the scales. © 2002 Society of Photo-Optical Instrumentation Engineers. [DOI: 10.1117/1.1428740]

Subject terms: motion; block matching; Markov random fields; multiresolution; eyelid movements.

Paper 010128 received Apr. 9, 2001; revised manuscript received July 19, 2001; accepted for publication July 20, 2001.

1 Introduction

This research was carried out within the framework of a medical application, where we are particularly interested in the movement of the eyelid. This area is not entirely structured, and the speed of the eyelid is not homogenous. The motion characterization must be sufficiently accurate to take into account these two properties. The movement observation is done on a sequence of gray level images. In addition, the movements present great differences in amplitude, and the low acquisition rate makes the motion estimation of large amplitudes difficult. A motion is considered as a motion of large amplitude when it exceeds three or four pixels per frame. There are a lot of techniques of movement estimation, but generally they are classified in three main categories: differential methods^{1,2} (methods of Horn, Schunk, and Nagel), mapping methods^{3,4} (block matching), and transform methods^{5,6} (Gabor transform, Fourier transform). The first methods give good results, provided that only movements of small amplitude are considered. The second techniques operate correctly on structured elements and motions of different amplitudes, nevertheless the precision of this process is not a subpixel one. The last methods are exploitable only for elementary movements. In our case, movements have various amplitudes. So a simple and efficient method to compute motion estimation for a large range of speed is proposed. The complement of differential methods and block matching allows us to characterize all the movements in image sequences. The cooperation of these two methods is achieved by a multiresolution strat-

egy. Section 2 summarizes the results of the theory of Markov random fields model and the principle of block matching applied to motion estimation. Components of the multiresolution strategy are explained in detail as a preamble to the algorithm in Sec. 3. In the last section a few results are presented.

2 Motion Estimate

2.1 Markov Random Fields

In this section, some results of Markov random fields (MRFs)⁷⁻⁹ applied to motion estimation are presented. These results are obtained from the Gibbs field model and Hammersley Clifford theorem. The central assumption is that the luminance of a pixel is constant in two successive images, although some works take into account variation luminance.¹⁰ Therefore, MRF modeling is equivalent to an energy function, and the motion estimation problem is reduced to the minimization of this energy function. Classically, the energy function is composed of two parts. The first one is the data energy:

$$[f(s + p_s^t, t + dt) - f(s, t)]^2,$$

where f is an image sequence. The latter is the regularization energy, based on the Tikhonov regularization model usually used for motion estimation:

$$V(s, s_j, p, p_j) = \beta \|p_s^t - p_{s_j}^t\|^2,$$

where $V()$ is the potential function, s is the current site, s_j is a set of sites in the neighborhood of s , and p_s^t is the motion vector on the site s at the time t . Its components are u_s and v_s . β is the parameter of regularization, varying from zero to infinity.

Concerning the choice of β , small values lead to an accurate solution for image data, but results are sensitive to noise. On the other hand, high value implies smooth solution, but results do not match the luminance data. Nevertheless, detection of movement of subpixel amplitude requires a small value for β . The best compromise between detection of the small movements of the eyelid and elimination of the noise of the acquisition system has to be found.

$$u_s = \frac{-2(2f_x\dot{f} + \sum_{\{s,s_j\} \in C_2} -2\beta u_{s_j}) \times [(f_y)^2 + 4\beta] + (2f_y\dot{f} + \sum_{\{s,s_j\} \in C_2} -2\beta v_{s_j}) \times (2f_x f_y)}{4[(f_x)^2 + 4\beta] \times [(f_y)^2 + 4\beta] - (2f_x f_y)^2}$$

$$v_s = \frac{-2(2f_y\dot{f} + \sum_{\{s,s_j\} \in C_2} -2\beta v_{s_j}) \times [(f_x)^2 + 4\beta] + (2f_x\dot{f} + \sum_{\{s,s_j\} \in C_2} -2\beta u_{s_j}) \times (2f_x f_y)}{4[(f_x)^2 + 4\beta] \times [(f_y)^2 + 4\beta] - (2f_x f_y)^2}$$

where u_s and v_s are the components of p_s^t

$$f_x = f(x + dx, y, t) - f(x, y, t);$$

$$f_y = f(x, y, + dy, t) - f(x, y, t);$$

$$\dot{f} = f(x, y, t + 1) - f(x, y, t).$$

The expression of $p_s(u_s, v_s)$ is a function of space luminance, temporal gradients, and the speed of the neighbors of the considered pixel. The value of $p_s(u_s, v_s)$ is obtained by an iterative process that converges toward the final value. The estimation of movement by MRF is finally reduced to u_s and v_s computing. All small movements are estimated with this simple calculation. Unfortunately, this method leads to incoherent results for great amplitude movements.

2.2 Block Matching Process

The estimation of motion by block matching⁴ consists (choosing a block in an image) in finding the best similar block with respect to criterion in another reference image. The displacement vector is deduced from the positions of the two blocks. The criterion of similarity between two blocks is generally the quadratic error or difference in absolute value. In our case, the criterion is defined as following:

$$C = \sum_B |(I_1 - \bar{I}_1) - (I_2 - \bar{I}_2)|,$$

where I_1 and I_2 are the pixel luminances of blocks, respectively, in the previous image and in the current image. \bar{I}_1

The total energy function is equal to:

$$E(s, t) = [f(s + p_s^t, t + dt) - f(s, t)]^2 + \sum_{\{s,s_j\} \in C_2} \beta \|p_s^t - p_{s_j}^t\|^2,$$

where C_2 is the second order clique.

The minimum energy function is obtained when the derivative from u_s and v_s is equal to zero, assuming that only a small displacement is taken into account.

The solution is $p_s = (u_s, v_s)$ with

and \bar{I}_2 are the average pixel luminances of blocks, respectively, in the previous image¹¹ and in the current image. B is the subset of pixels of the block.

The search for the reference block is done within a window whose dimensions are selected according to the detected displacement between the current image and reference image. The strategies of search are numerous; we can quote the binary searching, searching in spiral, or the hierarchical searching.

The block matching allows the estimation of great amplitude movement if initialization and correlation criterion are correctly chosen. Moreover, the size of the search are must be in relation to motion amplitude.

3 Method

It was shown in a preceding section that estimation of the optical flow by MRFs allows only a detection of small movements of amplitude less than 3 pixels, and that block matching detects movements of greater amplitudes if the process of search is well initialized. A multiresolution approach is used to merge these two methods.^{12,13} Indeed, if a movement is significant on scale 0 (initial image), it will become a movement of low amplitude in scales of coarser resolution. The MRF is used to characterize this small displacement, and motion tracking across the scale is achieved by BMP. BMP initialization is obtained with MRF. This section is organized as follows. First, the pyramidal framework is described, then the propagation of movement estimation across scales and BMP parameters are exposed. Finally our algorithm is presented.

3.1 Components of Pyramidal Approach

3.1.1 Pyramid construction

Pyramid construction is an efficient alternative to obtaining an adaptable motion estimate algorithm. Many multiresolu-

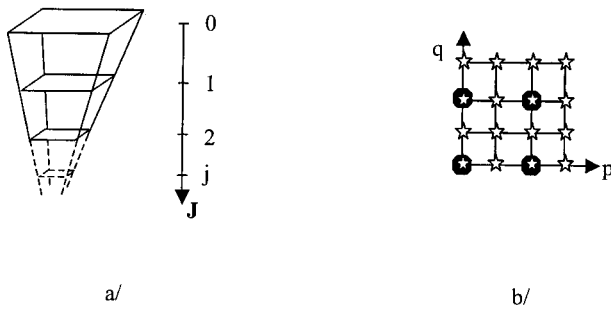


Fig. 1 (a) Image pyramid construction. (b) Scale $j+1$ is obtained from scale j . Scale j is composed of 16 pixels of \star . The four black reference mark pixels \bullet (p even and q even) represent the scale $j+1$.

tion schemes¹⁴⁻¹⁶ have been developed over the last few years. These methods are mainly optimized in regard to details needed to obtain the scale j from the scale $j+1$. We can quote criteria like entropy and aliasing. In this work, no study has been conducted to choose the best multiresolution method. However, precaution to limit aliasing has been taken by smooth filtering. The construction of the image pyramid is a fine to coarse process. A pixel at scale $j+1$ is simply the mean of its 4-neighborhood at scale j . The scale image $j+1$ of the pyramid is obtained by subsampling. If $m \times m$ is the number of pixels of the image 0, the size of the image j is $(m/2^j) \times (m/2^j)$ (Fig. 1). An image at resolution j will be denoted I_j .

3.1.2 Propagation of movement estimation

The movement estimation is carried out in a coarse to fine approach,¹⁷ as shown in Fig. 2(a). The difficulty of the coarse to fine approach is associating information points of scale $j+1$ to scale j . Indeed, we need to initialize movement image j on the base of movement estimation at scale $j+1$. Figure 2(b) shows how motion vectors of scale j are obtained from the motion vectors of scale $j+1$. Each motion vector for the pixels illustrated in black on scale j is two times the motion vector at scale $j+1$. All the other points at scale j are deduced from linear combinations, as shown in Fig. 2. Before presenting the algorithm, let us clarify the parameters of BMP.

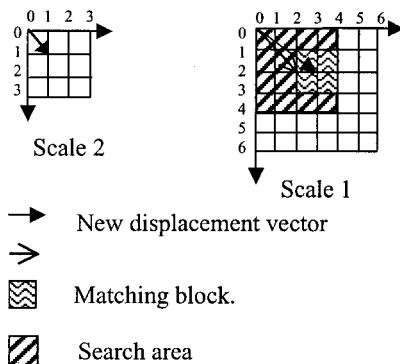


Fig. 3 Process of block matching across scales. In this example MRF initializes at scale 2. Propagation produces a vector magnified two times at scale 1. BMP improves accuracy of this vector at scale 1 and then at scale 0.

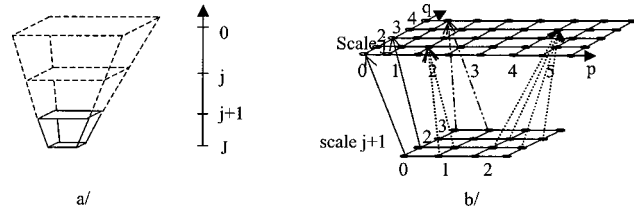


Fig. 2 (a) Movement pyramid creation: level 0 corresponds to the searched result. The algorithm begins at scale J . (b) Movement propagation: relation between pixels at scale $j+1$ and pixels at scale j are illustrated. New pixels at scale j are initialized by the interpolation of the neighboring values at scale $j+1$ (as illustrated).

3.1.3 Parameters of block matching

As previously shown, BMP consists in linking a block of an image to another one in another image. In this work, the chosen block size is 3×3 pixels. The search direction for matching is initialized at scale j by propagating the motion vector estimated by MRF at scale $j+1$. The size of the search area is hierarchical and depends on the motion vector determined at scale $j+1$. Indeed, if a displacement of q pixels at scale $j+1$ is detected, displacement on the upper scale will be of $2 \times q$ pixels. As defined before, the correspondence criterion is the mean difference of luminance pixel to pixel between the two blocks. The block minimizing this difference is selected. Figure 3 represents the way to track the motion across scales with BMP (in this example only three scales are represented).

The size of the search area is defined by the displacement vector estimated on the coarser scale. This area is centered on the pixel whose position is calculated with information from the lower scale. The size of the interest area is four times the value found on the coarse scale.

3.2 Algorithm

Let there be a temporal sequence of $(n+1)$ images

$$\{I^0, I^1, \dots, I^k, \dots\}_{k \in [0, n]},$$

where k denotes the time. First of all, a multiresolution pyramid of $(P^{k-1}, P^k)_{k \in [0, n]}$ is built following the process

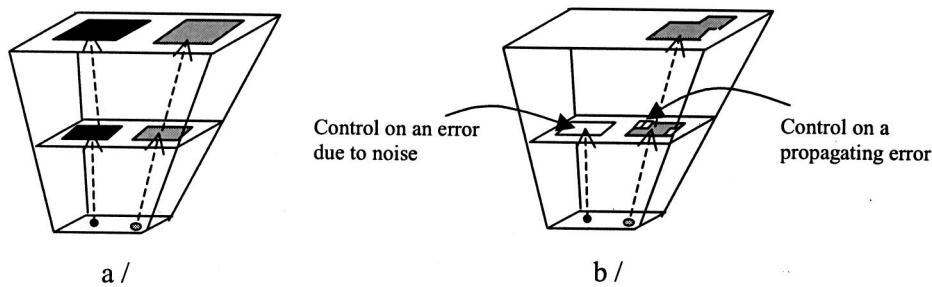


Fig. 4 Interest of control: (a) propagation of information without control, the error is propagated and (b) propagation of information with control, to eliminate error. The gray pixel is where motion is detected by the Markov process. ● pixel is where false motion due to noise is detected by MRF. The gray square set of pixels is where block matching is applied, the ■ set of pixels is where block matching is applied, and the □ set of pixels is forced to 0.

described in Sec. 3.1.1. All calculations will be carried out on a pair of successive pyramids noted (P^{k-1}, P^k) where:

$$P^{k-1} = \{I_0^{k-1}, I_1^{k-1}, \dots, I_j^{k-1}\} \text{ and } P^k = \{I_0^k, I_1^k, \dots, I_j^k\}$$

with $J+1$ the number of scales. The task of the movement estimation algorithm is to build gradually the pyramid of movement:

$$\{(U^k_j, V^k_j), (U^k_{j-1}, V^k_{j-1}), \dots, (U^k_0, V^k_0)\},$$

where (U^k_0, V^k_0) is the expected movement vector image. The algorithm is organized as following:

1. For each pyramid image, movement estimation is processed by MRF on the coarsest scale (I_j^{k-1}, I_j^k) and produces vector image $(U^k_{j=j}, V^k_{j=j})$.
2. Vectors are propagated on the next finer scale, as explained in Sec. 3.1.2 to initialize (U^k_j, V^k_j) with $j = j - 1$.
3. At the finer scale, two configurations are possible to refine (U^k_j, V^k_j) : the initial vector is null, and in this case the motion vector is determined by MRF, or a nonnull initial vector is found and used to initialize the BMP whose parameters are defined in Sec. 3.1.3.
4. The algorithm is iterated from step 2 until scale 0. The final result is the vector image (U^k_0, V^k_0) .

To improve the process, a modification in step 3 is introduced. If motion is detected for a given point at scale $j + 1$, the initial vectors at scale j will not be null in the 4-neighborhood. Consequently, all these points are checked to know if they correspond to real movement. So, before estimation by the block matching, the propagation of movement is refined by MRF. If a point does not correspond to movement, its initialization is forced to 0. Figure 4 illustrates the utility of control before the application of block matching on the same example. Figure 5 shows an example of two image pyramids where the complement of MRF and BMP is clear. The algorithm is summarized in Fig. 6.

4 Some Experimental Results

Results are presented for synthetic and real sequences. In particular, the robustness of the method against the noise is

shown, then its behavior on movements of various amplitudes is illustrated. A comparison between the results obtained with the cooperative method and the results obtained with MRF or BMP applied separately is presented. Finally, some quantitative movement estimates are presented.

4.1 Noise Effect

Real images are corrupted by the noise of the acquisition system. At first, the noise of the acquisition system is estimated. This system includes optic, CCD, and electronic. This noise is classically modeled by a Gaussian distribution, and the estimation of the mean variance is achieved from the image sequence of homogeneous luminance with different gray levels. Measure gives a value of 3 for the variance. Subsequently, the robustness of the algorithm is evaluated on noisy synthetic images. This test permits the adjustment of parameters, mainly β .

A pair of images extracted from the test sequence is shown in Fig. 7. The sequence of images represents an homogeneous square moving in translation on an homogeneous background (whose luminance is different from the square luminance). The movement is a translation of one pixel to the right according to the horizontal axis. The results are consigned in Fig. 8.

The results in Fig. 8(a) show that the detection of movement is correct. For a noisy sequence with Gaussian noise of variance similar to the noise of acquisition system, some vectors present false directions and wrong norms. Obviously, the overall movement estimation is satisfactory [Fig. 8(b)]. As noise variance increases, the result is degrading

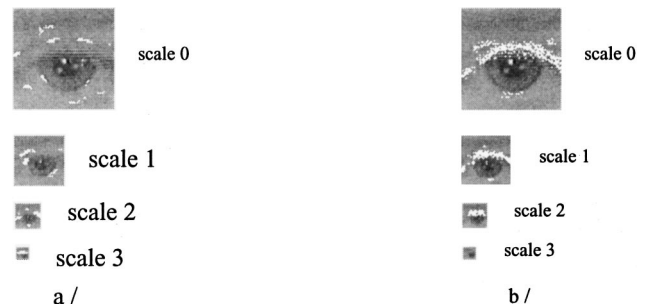


Fig. 5 Contributions of (a) the Markovian approach and (b) of block matching. The white points show the pixels where motion is detected.

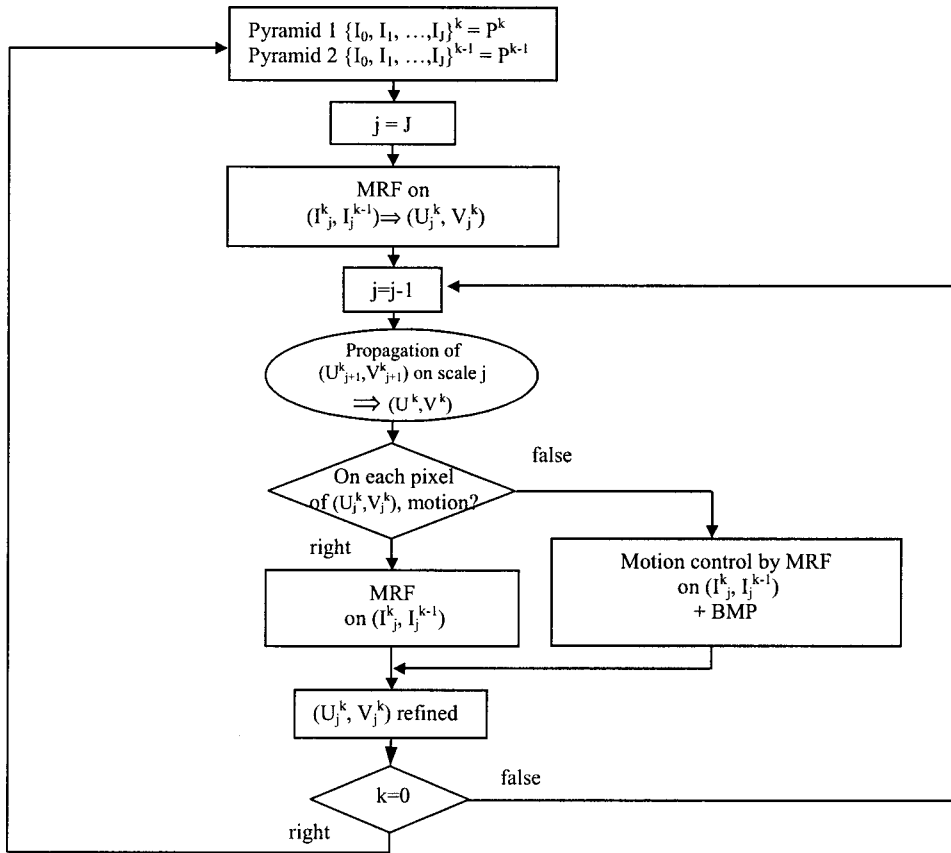


Fig. 6 Algorithm for motion estimate. Notation: the I image of the sequence, (U_j^k, V_j^k) motion vector at time k and scale j .

and it becomes difficult to localize good vectors among wrong ones [Fig. 8(c)]. We still recognize the dominating movement, but it seems unreasonable to calculate the norm of the motion vectors to determine the speed of the object. Experiments and settings have been conducted and show that the algorithm will not be sensitive to noise added by the acquisition system.

4.2 Speed Estimate

An homogeneous disk with a colored sector has been designed to study the behavior of our algorithm for movements of various amplitudes along the image sequence

(corresponding to various speeds). Then this disk in uniform rotation (angular velocity $\pi/3$ rd/s) has been shot at 25 images/s.

Figure 9(c) shows that norm of vectors decreases near the center of the disk. In Fig. 10, the contribution of MRF and BMP across the scale is clearly shown. On each scale MRF allows the detection of small displacements, and BMP tracks the movements that are detected by MRF on the coarser scale.

Movements with large amplitude are detected in the coarsest scales. As the amplitude of movement decreases (near the center of the disk), the estimate is initialized at the finest scales. The efficiency of our algorithm is evaluated

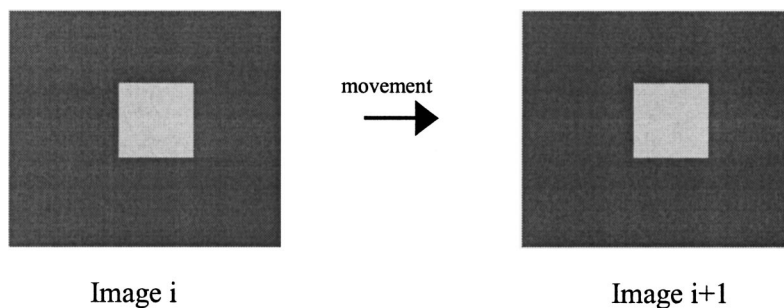


Fig. 7 Two successive images of the sequence.

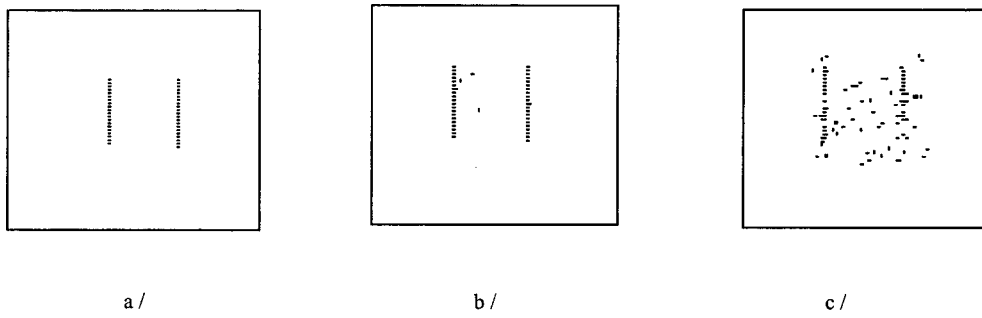


Fig. 8 Displacement vectors (a) on the initial sequence without noise, (b) on the sequence with noise (noise variance=4), and (c) on the sequence with noise (noise variance=9).

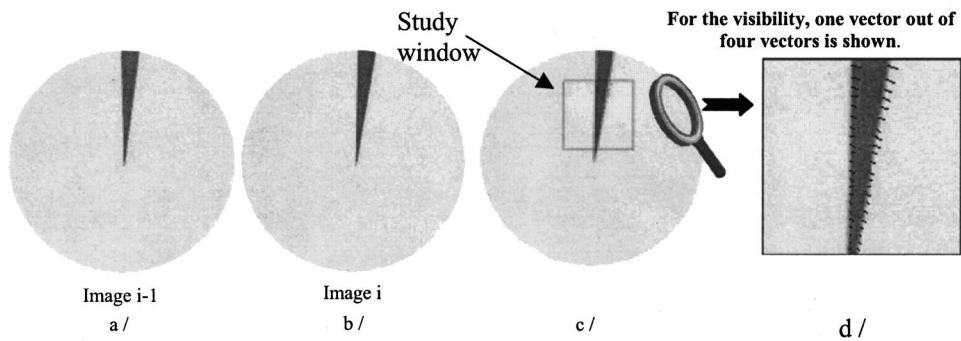


Fig. 9 (a) and (b) Pair of images extracted from the sequence, and (c), (d) the displacement vector field associated.

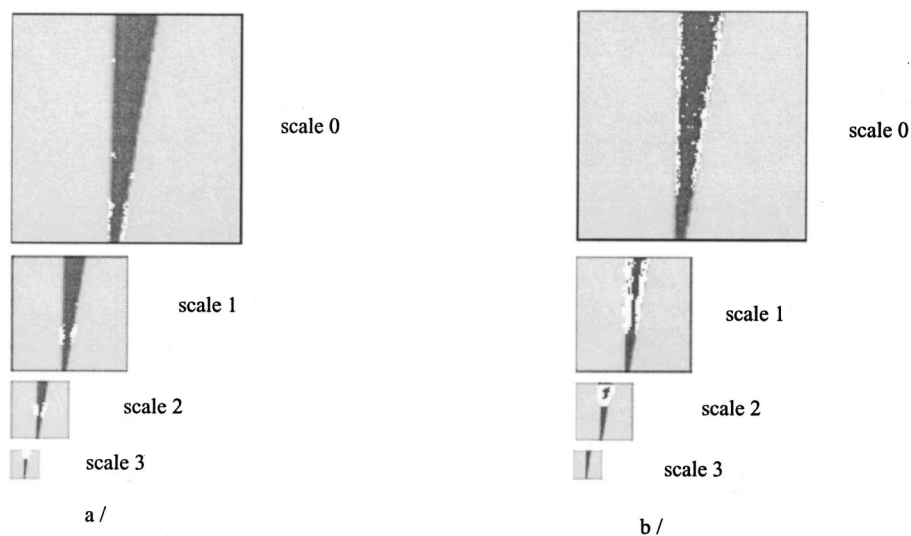


Fig. 10 Contribution at different scales of (a) the Markovian approach, and (b) block matching. The white points show pixels over which motion is detected (video rate: 25 images/s).

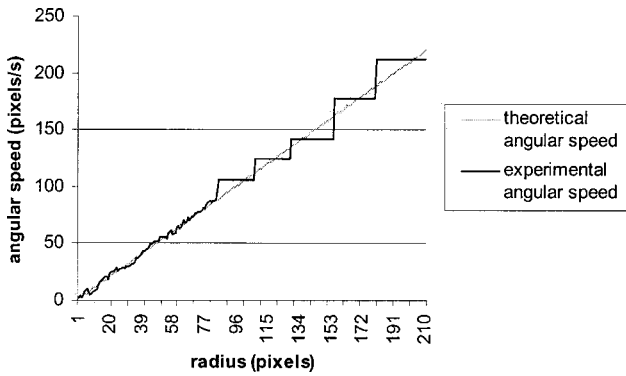


Fig. 11 Comparison between theoretical and experimental angular speed. The curve is composed of two parts corresponding to the Markov method and the block matching process. The speed increases by 1 pixel/s when the radius increases by 23 pixels. Motion estimation by Markov random fields is subpixel, consequently the experimental curve is similar to the theoretical one. The motion estimation using the block matching process is constant at intervals of 23 pixels, because the block matching process has a resolution of one pixel (video rate: 25 images/s).

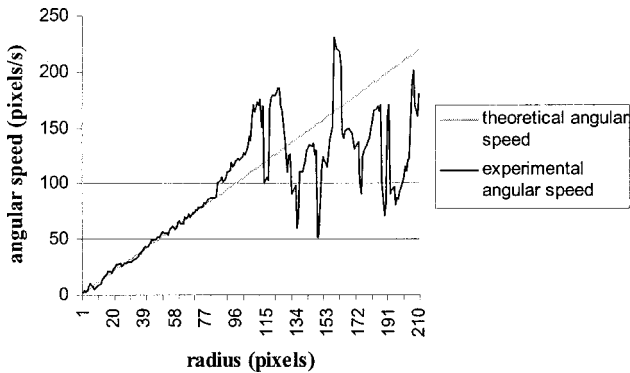


Fig. 12 Comparison between theoretical and experimental angular speed. The MRF results are similar to the theoretical ones only for small displacement. Thus the difference between the two curves is important.

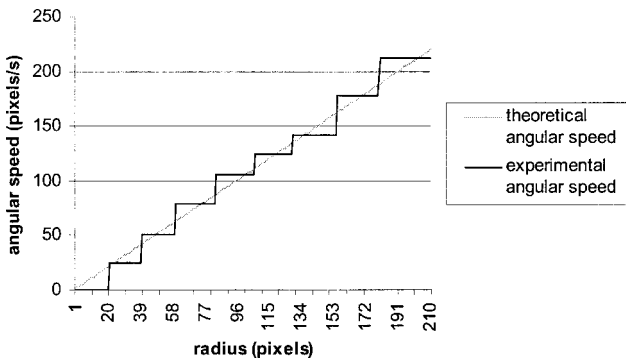


Fig. 13 Comparison between theoretical and experimental angular speed. The BMP cannot provide estimation for motion slower than 25 pixels/s. The curve for the BMP is step-like, but the estimate is close to the theoretical angular speed.

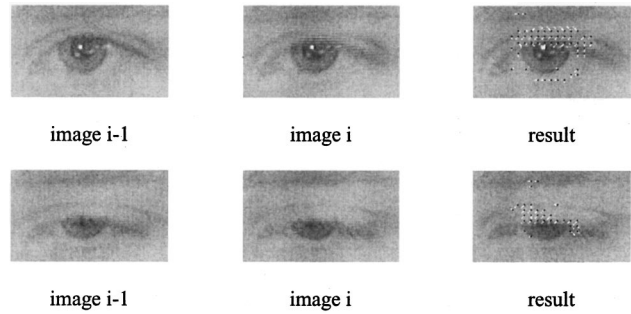


Fig. 14 Images and results for voluntary eyelid closure. For visibility, only one vector out of four is shown. Horizontal aliasing is due to interlacing.

using the comparison between experimental and theoretical angular speeds (Fig. 11).

4.3 Comparison of Results Obtained with Different Methods

In the last section, the previous example (a disk in uniform rotation) is used to show the efficiency of the MRF and BMP cooperation. The cooperative method is compared to the MRF or BMP method applied separately.

Figure 12 presents theoretical and MRF results. The MRF method gives good results only for small displacements. Motion amplitudes greater than two or three pixels per image lead to unstable estimation; the deterministic algorithm used in this approach can converge toward a global minimum only when dealing with small movements.

Figure 13 illustrates theoretical and BMP results. The step-like shape is due to the one pixel resolution linked to the fact that BMP cannot provide an estimation for motion slower than 25 pixels/s (video rate is 25 images/s). But the estimate stays close to the theoretical angular speed.

Figure 11 presents the MRF and BMP cooperation. This method takes the advantage of each process. For small displacements, the MRF process is used for its greater accuracy. For large displacements BMP is used for its capability to detect large movement with a correct and stable estimate.

4.4 Examples of Application on a Deformable Area

Figure 14 presents two pairs of images showing the voluntary eyelid closure. The algorithm seems reliable for the determination of the direction and norm of the motion vectors. Some estimation errors are due to noise and aliasing, and they will be eliminated in future experimentation with a full frame camera. A solution to cope with the noise problem would be to increase the value of β , which would imply the disappearance of false vectors. However, as specified in Sec. 2.1, if β is too much increased, noise but also small movement vectors will be removed.

The speed of the eyelid is more significant at its beginning than at its end (Fig. 15). For each person the speed of the eyelid is different, and can even vary for the same person according to her tiredness or her nervousness and the voluntary or involuntary nature of the movement, so we give just a speed range. These values were obtained with test sequences in a laboratory. It is probable that the found eyelid speed range should be modified if the values were derived from a large number of persons. Finally, these val-

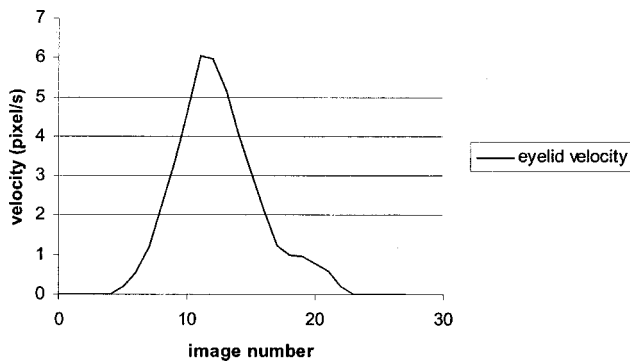


Fig. 15 Curves depicting the eyelid velocity (video rate: 200 images/s). The movement seems to feature two phases.

ues, in their current units (pixels/s), depend on the experimental conditions of acquisition (resolution of the sensor, lens, object/camera distance, and video rate). The experiment seems to point out two phases (Fig. 15) in eyelid movement: beginning and middle courses of eyelid movement, where acceleration and then deceleration are regular; and the end of eyelid movement, which present a different speed evolution. Further experiments will be made to confirm these observations.

5 Conclusion

A multiresolution scheme for the cooperation of two different approaches in motion estimation has been presented. These two approaches are Markov field and block matching. The resulting method is able to estimate various amplitudes of motion in the image sequence. The minimum of motion depends on the trade-off between motion and noise, while the maximum of motion detected depends on the depth J of the multiresolution pyramid. The smallest detected movement is subpixel displacement, and the largest one is equal to about 2^{J+1} . Presented examples clearly show the contribution of each of the two detection methods. The multiresolution method can be applied to the object motion estimate as well as to the estimate of motion on deformable surfaces. In this work, application of the method has been conducted for estimate of the movement of the eyelid. Automation of the measures of the movement of the eyelid closing and opening are in progress. Perspectives concern the study of the value of regularization parameters and the construction of a multiscale pyramid.

Acknowledgment

This work was supported by A.N.V.A.R. Bourgogne France.

References

1. H. N. Nagel, "On the estimation of optical flow: Relations between different approaches and some new results," *Artif. Intel.* **33**, 299–324 (1987).
2. B. K. Horn and B. G. Schunck, "Determining optical flow," *Artif. Intel.* **17**, 185–183 (1981).
3. B. C. Song and J. B. Ra, "A fast multi-resolution block matching algorithm for motion estimation," *Signal Process. Image Commun.* **15**(9), 799–810 (2000).
4. C. Alexandre and H. Vu Thien, "Fast motion estimation algorithm," *Traitement du Signal* **13**(4), 351–359 (1996).
5. A. Spinei, D. Pellerin, and J. Héroult, "Spatiotemporal energy-based method for velocity estimation," *Signal Process.* **65**(3), 347–362 (1998).
6. D. Vernon, "Computation of instantaneous optical flow using the phase of Fourier components," *Image Vis. Comput.* **17**(3–4), 189–199 (1999).
7. F. Heitz, P. Perez, and P. Bouthemy, "Constrained multiscale Markov random fields and the analysis of visual motion," *Publication Interne de l'IRISA* **627**, 1–40 (1992).
8. F. Heitz and P. Bouthemy, "Multimodal estimation of discontinuous optical flow using Markov random fields," *IEEE Trans. Pattern Anal. Mach. Intell.* **15**(12), 1217–1232 (1993).
9. M. Kardouchi, "Contribution à l'étude du mouvement avec les champs de Markov: Régularisation et prise en compte des discontinuités," PhD Thesis, Univ. Bourgogne, Dijon (1998).
10. J. C. Pesquet, "Motion estimation in the presence of illumination variations," *Signal Process. Image Commun.* **16**, 373–381 (2000).
11. P. Fua, "Combining stereo and monocular information to compute dense depth maps that preserve depth maps discontinuities," *Proc. Int. Joint Conf. Artificial Intell.*, pp. 1292–1298, Sydney, Australia (1991).
12. P. Anandan, "A computational framework and an algorithm for the measurement of visual motion," *Int. J. Comput. Vis.* **2**, 283–310 (1989).
13. S. Zafar, Y. Zhang, and B. Jabbari, "Multiscale video representation using multiresolution motion compensation and wavelet decomposition," *IEEE J. Sel. Areas Commun.* **11**(1), 24–35 (1993).
14. P. J. Burt and E. H. Adelson, "The Laplacian pyramid as a compact image code," *IEEE Trans. Commun.* **31**, 532–540 (1983).
15. A. Aldroubi and M. Unser, "Families of multiresolution and wavelet spaces with optimal properties," *Numer. Funct. Anal. Optimiz.* **14**(5), 417–446 (1993).
16. M. Unser, A. Aldroubi, and M. Eden, "A family of polynomial spline wavelet transforms," *Signal Process.* **30**(2), 141–162 (1993).
17. R. Leconge, O. Lalignant, and F. Truchetet, "Markov random fields and block matching for multiresolution motion estimation," *Proc. SPIE* **3968**, 10–21 (2000).

Rémy Leconge received the DEA degree from Université de Bourgogne, France, in 1999. He is currently working toward the PhD degree. His major areas of interest are image processing and motion tracking.

Olivier Lalignant received his PhD degree in 1995 from the Université de Bourgogne, France. He is an assistant professor in the computing, electronic, imaging department (Le2i) at Université de Bourgogne, France. His research interests are focused on multiscale edge detection, merging of data, wavelet transform, and recently motion estimation.

Frédéric Truchetet received the master degree in physics at Dijon University, France, in 1973 and a PhD in electronics at the same university in 1977. He was with Thomson-CSF for two years as a research engineer and he is currently full professor and the head of the image processing group at Le2i, Laboratory of Electronic, Computer, and Imaging Sciences, at Université de Bourgogne, France. His research interests are focused on image processing for artificial vision inspection and particularly on wavelet transforms, multiresolution edge detection, and image compression. He is member SPIE, IEEE, and ISIS (a research group of CNRS).

Alain Diou received the engineer's degree in electronics at Nancy University, France, in 1968, an engineering doctorate in medical electronics in 1972, and received the doctor of science in 1983 at the same university in hybrid computing domain. He is currently full professor in the image processing group at Le2i, Laboratory of Electronic, Computer, and Imaging Sciences, at Université de Bourgogne, France. His research interests are focused on image processing for artificial vision and particularly on multiresolution region segmentation and image compression.